

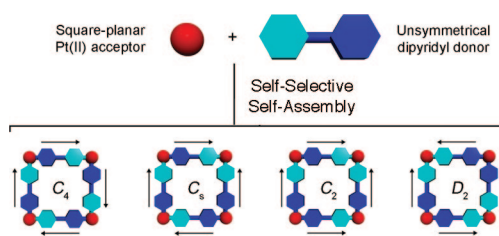
Self-Selection in the Self-Assembly of Isomeric Supramolecular Squares from Unsymmetrical Bis(4-pyridyl)acetylene Ligands

Liang Zhao,[†] Brian H. Northrop,[†] Yao-Rong Zheng,[†] Hai-Bo Yang,[†] Hyo Jin Lee,[‡] Young Min Lee,[‡] Joo Yeon Park,[‡] Ki-Whan Chi,^{*,‡} and Peter J. Stang^{*,†}

Department of Chemistry, University of Utah, 315 South 1400 East, Room 2020, Salt Lake City, Utah 84112, and Department of Chemistry, University of Ulsan, Ulsan 680-749, Republic of Korea

kwchi@mail.ulsan.ac.kr; stang@chem.utah.edu

Received May 4, 2008



A new approach wherein steric interactions between substituents of unsymmetrical bis(4-pyridyl)acetylene ligands dictate the self-selection of single isomers of [4 + 4] self-assembled squares is presented. Each [4 + 4] self-assembly is characterized by multinuclear ³¹P and ¹H NMR spectroscopies and electrospray ionization mass spectrometry. NMR spectroscopic studies are used to provide a means of evaluating the efficiency of bulky substituents at proximal or remote positions relative to the Pt–N bonding motif to direct self-selection. Molecular modeling using the MMFF force field is utilized to determine the relative energy of different isomers of each assembly, and modeling results reasonably explain the trend in self-selectivity with varying pyridyl substitution.

Introduction

The rational design and synthesis of discrete metallocupramolecular architectures is of intense interest due to the fascinating structural diversity and potential applications of these novel functional materials.^{1,2} By using the common, directional bonding geometries of transition metal centers—typically octahedral, square planar or tetrahedral—in combination with a

variety of organic nucleophilic ligands of specific geometry and size, a wealth of nanometer-sized supramolecular polygons and polyhedra can be successfully obtained via the bottom-up synthetic approach.^{1,3} Multiple examples of coordination-driven self-assembly rely upon the use of symmetric dipyriddy ligands together with Pd(II) and Pt(II) building blocks to construct a range of supramolecular architectures.^{4,5} So far, few studies have investigated the use of unsymmetrical dipyriddy ligands⁶ to construct discrete supramolecules.

[†] University of Utah.

[‡] University of Ulsan.

(1) (a) Stang, P. J.; Olenyuk, B. *Acc. Chem. Res.* **1997**, *30*, 502–518. (b) Leininger, S.; Olenyuk, B.; Stang, P. J. *Chem. Rev.* **2000**, *100*, 853–908. (c) Seidel, S. R.; Stang, P. J. *Acc. Chem. Res.* **2002**, *35*, 972–983. (d) Fujita, M. *Chem. Soc. Rev.* **1998**, *27*, 417–425. (e) Swiegers, G. F.; Malefetse, T. J. *Chem. Rev.* **2000**, *100*, 3483–3537. (f) Holliday, B. J.; Mirkin, C. A. *Angew. Chem., Int. Ed.* **2001**, *40*, 2022–2043. (g) Cotton, F. A.; Lin, C.; Murillo, C. A. *Acc. Chem. Res.* **2001**, *34*, 759–771. (h) Fujita, M.; Tominaga, M.; Hori, A.; Therrien, B. *Acc. Chem. Res.* **2005**, *38*, 369–378. (i) Fiedler, D.; Leung, D. H.; Bergman, R. G.; Raymond, K. N. *Acc. Chem. Res.* **2005**, *38*, 349–358. (j) Severin, K. *Chem. Commun.* **2006**, 3859–3867. (k) Pitt, M. A.; Johnson, D. W. *Chem. Soc. Rev.* **2007**, *36*, 1441–1453.

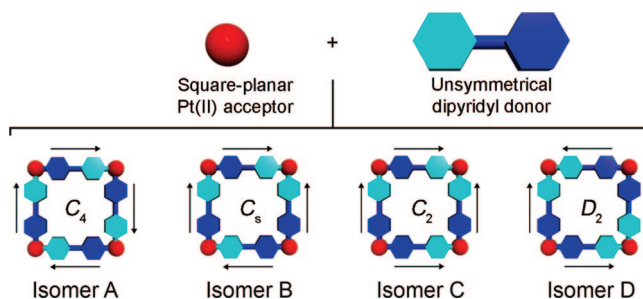
(2) (a) Cotton, F. A.; Lin, C.; Murillo, C. A. *J. Am. Chem. Soc.* **2001**, *123*, 2670–2671. (b) Yoshizawa, M.; Takeyama, Y.; Kusukawa, T.; Fujita, M. *Angew. Chem., Int. Ed.* **2002**, *41*, 1347–1349. (c) Murase, T.; Sato, S.; Fujita, M. *Angew. Chem., Int. Ed.* **2007**, *46*, 1083–1085. (d) Balzani, V.; Bergamini, G.; Campagna, S.; Puntoriero, F. *Top. Curr. Chem.* **2007**, *280*, 1–36. (e) Yang, H.-B.; Ghosh, K.; Zhao, Y.; Northrop, B. H.; Lyndon, M. M.; Muddiman, D. C.; White, H. S.; Stang, P. J. *J. Am. Chem. Soc.* **2008**, *130*, 839–841.

(3) (a) Caulder, D. L.; Raymond, K. N. *Angew. Chem., Int. Ed. Engl.* **1997**, *36*, 1440–1442. (b) Stang, P. J. *Chem. Eur. J.* **1998**, *4*, 19–27. (c) Gianneschi, N. C.; Tiekink, E. R. T.; Rendina, L. M. *J. Am. Chem. Soc.* **2000**, *122*, 8474–8479. (d) Tabellion, F. M.; Seidel, S. R.; Arif, A. M.; Stang, P. J. *J. Am. Chem. Soc.* **2001**, *123*, 7740–7741. (e) Iengo, E.; Zangrando, E.; Minatel, R.; Alessio, E. *J. Am. Chem. Soc.* **2002**, *124*, 1003–1013. (f) Campbell, K.; Kuehl, C. J.; Ferguson, M. J.; Stang, P. J.; Tykwinski, R. R. *J. Am. Chem. Soc.* **2002**, *124*, 7266–7267. (g) Iengo, E.; Zangrando, E.; Geremia, S.; Graff, R.; Kieffer, B.; Alessio, E. *Chem. Eur. J.* **2002**, *8*, 4670–4674. (h) Su, C.-Y.; Cai, Y.-P.; Chen, C.-L.; Smith, M. D.; Kaim, W.; Zur Loye, H.-C. *J. Am. Chem. Soc.* **2003**, *125*, 8595–8613. (i) Addicott, C.; Das, N.; Stang, P. J. *Inorg. Chem.* **2004**, *43*, 5335–5338. (j) Natarajan, R.; Savitha, G.; Moorthy, J. N. *Cryst. Growth Des.* **2005**, *5*, 69–72. (k) Steel, P. J. *Acc. Chem. Res.* **2005**, *38*, 243–250. (l) Yang, H.-B.; Ghosh, K.; Northrop, B. H.; Stang, P. J. *Org. Lett.* **2007**, *9*, 1561–1564. (m) Yamaguchi, T.; Tashiro, S.; Tominaga, M.; Kawano, M.; Ozeki, T.; Fujita, M. *Chem. Asian J.* **2007**, *2*, 468–476. (n) Wang, Y.; Cheng, P.; Song, Y.; Liao, D.-Z.; Yan, S.-P. *Chem. Eur. J.* **2007**, *13*, 8131–8138.

Statistically, unsymmetrical dipyrindyl ligands would give rise to a mixture of isomers as a result of random combinations of different orientations of ligands provided that there is no driving bias, such as specific molecular information or interactions encoded in or between the building blocks that would lead to self-sorting.⁷ It is a formidable challenge, therefore, to control and isolate one single, pure isomer of a self-assembled metallacycle that contains an unsymmetrical ligand as one of its building units.^{6,8} Our group has previously reported the preferential self-assembly of a single [2 + 2] rhomboidal isomer from ambidentate pyridyl/carboxylate donor ligands when combined with 90° or 0° ditopic organoplatinum acceptors.⁹ Exclusive self-selectivity resulted from a combination of geometric and electronic factors: in each case the rhomboid isomer that was the least geometrically strained and had the greatest separation of charge was the only isomer formed. This charge separation approach has been further extended to include the exclusive [3 + 3] self-assembly of one isomer of a heterobimetallic Pd₃–Fe₃ triangle via the coordination of a singular, ambidentate 4-isonicotinate ligand.¹⁰ This method of relying on charge–charge interactions and geometric strain, however, is likely to reach its limit upon the exploration into larger self-assemblies given that charge–charge interactions decrease with the square of their separation and larger systems are better able to distribute and therefore tolerate geometric strain. Herein, we describe a new strategy for the self-selection of a single isomer of a [4 + 4] supramolecular square composed of four 90° Pt(II) acceptors and four substituted, unsymmetrical bis(4-pyridyl)acetylene ligands. The self-selection process is governed by steric and electronic interactions.

Among the many 2D supramolecular polygon geometries, supramolecular squares have been extensively studied as they can be easily prepared using square-planar Pd(II) and Pt(II) metal centers as 90° corner units.^{1b,f,11} Typically, such square-planar Pd(II) or Pt(II) metals are combined with symmetrical

SCHEME 1. Schematic Representation of the Self-Assembly of Four Pt(II) Acceptors with Four 180° Unsymmetrical Dipyrindyl Donors To Make Four Kinds of Isomeric Supramolecular Squares^a



^a The asymmetry of the dipyrindyl donor is reflected in the two shades of blue. Point group symmetries of each supramolecular square are given. Arrows are drawn around the perimeter of each metallacycle to further aid in visualizing the different orientations of the unsymmetrical donors in each isomer.

donor ligands, such as linear dipyrindyl donors, to produce identical discrete supramolecular metallacycles. Discrete metallacycles may still be formed when unsymmetrical donor ligands are used; however they are considerably less likely to be identical. As a general model, one can envision an unsymmetrical, linear dipyrindyl ligand as shown in Scheme 1. Both electron-rich pyridyl moieties are depicted as blue hexagons, however the two pyridyl moieties are colored different shades of blue to reflect their asymmetry. In the absence of any biasing interactions, there are four different isomers that may be formed upon the self-assembly of supramolecular [4 + 4] squares from an unsymmetrical ditopic donor and a 90° Pt(II) acceptor unit, depicted as a red sphere. The four different squares are shown as isomers A–D in Scheme 1. Isomer A, for example, has all four unsymmetrical donors oriented in an alternating fashion such that one of each type of pyridyl moiety, one light blue and one dark blue, is coordinated with each Pt(II) center. The resulting [4 + 4] metallacycle has C_4 symmetry. In isomer B, one of the donor ligands is rotated 180° relative to isomer A, resulting in a supramolecular square with C_s symmetry. In this isomer, two of the Pt(II) acceptors will be coordinated by two different pyridyl moieties (one dark blue and one light blue, upper and lower left corners of B), while the remaining two Pt(II) acceptors are coordinated with two of the same pyridyl donors, either two light blue (upper right corner) or two dark blue (lower right corner). An analogous situation arises in isomer C; however, C is more symmetric than isomer B. This difference in symmetry results from the relative orientations of unsymmetrical donors in each [4 + 4] square, which gives isomer C a 2-fold axis of rotational symmetry. The final supramolecular square structure that can be made is isomer D, which has D_2 symmetry. In isomer D, every Pt(II) acceptor is coordinated by two of the same pyridyl moieties, either two dark blue or two light blue.

Along these lines, we have adopted the organoplatinum ligand *cis*-(Me₃P)₂Pt(OTf)₂ (**1**) as a 90° acceptor for constructing 2D square architectures because of its ditopic bonding motif and relatively simple proton NMR, the latter ensuring that the NMR spectra of resulting single or multiple isomers are discernible. We have also prepared three new unsymmetrical bis(4-pyridyl)-acetylene donors: 2,6-dimethyl-4-(4-ethynylpyridinyl)pyridine (**2**), 2-chloro-4-(4-ethynylpyridinyl)pyridine (**3**), and 3,5-dichloro-4-(4-ethynylpyridinyl)pyridine (**4**), which were synthesized via Sonogashira coupling reactions of their respective pyridyl

(4) (a) Yang, H.-B.; Das, N.; Huang, F.; Hawkrige, A. M.; Muddiman, D. C.; Stang, P. J. *J. Am. Chem. Soc.* **2006**, *128*, 10014–10015. (b) Yang, H.-B.; Hawkrige, A. M.; Huang, S. D.; Das, N.; Bunge, S. D.; Muddiman, D. C.; Stang, P. J. *J. Am. Chem. Soc.* **2007**, *129*, 2120–2129. (c) Yang, H.-B.; Ghosh, K.; Northrop, B. H.; Zheng, Y.-R.; Lyndon, M. M.; Muddiman, D. C.; Stang, P. J. *J. Am. Chem. Soc.* **2007**, *129*, 14187–14189. (d) Northrop, B. H.; Glöckner, A.; Stang, P. J. *J. Org. Chem.* **2008**, *73*, 1787–1794.

(5) (a) Suzuki, K.; Kawano, M.; Sato, S.; Fujita, M. *J. Am. Chem. Soc.* **2007**, *129*, 10652–10653. (b) Murase, T.; Sato, S.; Fujita, M. *Angew. Chem., Int. Ed.* **2007**, *46*, 5133–5136.

(6) Rang, A.; Engeser, M.; Maier, N. M.; Nieger, M.; Lindner, W.; Schalley, C. A. *Chem. Eur. J.* **2008**, *14*, 3855–3859.

(7) (a) Wu, A.; Isaacs, L. *J. Am. Chem. Soc.* **2004**, *126*, 10035–10043. (b) Liu, S.-M.; Ruscip, C.; Mukhopadhyay, P.; Chakrabarti, S.; Zavalij, P. Y.; Isaacs, L. *J. Am. Chem. Soc.* **2005**, *127*, 15959–15967. (c) Mukhopadhyay, P.; Zavalij, P. Y.; Isaacs, L. *J. Am. Chem. Soc.* **2006**, *128*, 14093–14102.

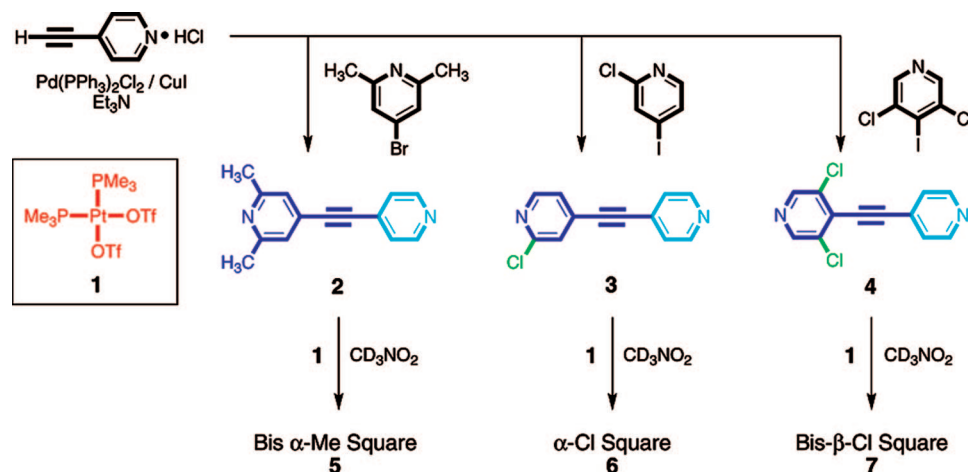
(8) (a) Barboiu, M.; Petit, E.; van der Lee, A.; Vaughan, G. *Inorg. Chem.* **2006**, *45*, 484–486. (b) Nitschke, J. R. *Acc. Chem. Res.* **2007**, *40*, 103–112. (c) Legrand, Y.-M.; van der Lee, A.; Barboiu, M. *Inorg. Chem.* **2007**, *46*, 9540–9547. (d) Hutin, M.; Cramer, C. J.; Gagliardi, L.; Shahi, A. R. M.; Bernardinelli, G.; Cerny, R.; Nitschke, J. R. *J. Am. Chem. Soc.* **2007**, *129*, 8774–8780. (e) Langner, A.; Tait, S. L.; Lin, N.; Rajadurai, C.; Ruben, M.; Kern, K. *Proc. Natl. Acad. Sci. U.S.A.* **2007**, *104*, 17927–17930.

(9) (a) Chi, K.-W.; Addicott, C.; Arif, A. M.; Stang, P. J. *J. Am. Chem. Soc.* **2004**, *126*, 16569–16574. (b) Chi, K.-W.; Addicott, C.; Moon, M.-E.; Lee, H. J.; Yoon, S. C.; Stang, P. J. *J. Org. Chem.* **2006**, *71*, 6662–6665.

(10) Ghosh, S.; Turner, D. R.; Batten, S. R.; Mukherjee, P. S. *Dalton Trans.* **2007**, 1869–1871.

(11) Some recent examples: (a) Janzen, D. E.; Patel, K. N.; VanDerveer, D. G.; Grant, G. J. *Chem. Commun.* **2006**, 3540–3542. (b) You, C.-C.; Hippus, C.; Gruene, M.; Wuerthner, F. *Chem. Eur. J.* **2006**, *12*, 7510–7519. (c) Ferrer, M.; Gutierrez, A.; Mounir, M.; Rossell, O.; Ruiz, E.; Rang, A.; Engeser, M. *Inorg. Chem.* **2007**, *46*, 3395–3406. (d) Ghosh, S.; Batten, S. R.; Turner, D. R.; Mukherjee, P. S. *Organometallics* **2007**, *26*, 3252–3255. (e) Blanco, V.; Chas, M.; Abella, D.; Peinador, C.; Quintela, J. M. *J. Am. Chem. Soc.* **2007**, *129*, 13978–13986. (f) Blanco, V.; Chas, M.; Abella, D.; Pfa, E.; Platas-Iglesias, C.; Peinador, C.; Quintela, J. M. *Org. Lett.* **2008**, *10*, 409–412.

SCHEME 2. Synthesis of Unsymmetrical Dipyriddy Donors 2–4 and Their Combination with 90° Pt(II) Acceptor 1 in CD₃NO₂ Leading to the Self-Assembly of Supramolecular Squares 5–7, Respectively



halides and 4-ethynylpyridine (Scheme 2). Mixing acceptor **1** with donors **2–4** in a 1:1 molar ratio results in the spontaneous self-assembly of supramolecular square compounds **5–7**, respectively, as shown in Scheme 2. Ditopic donors **2–4** were chosen because of the variation in the size and regiochemistry of substituents on their pyridyl rings. As outlined above, each unsymmetrical donor ligand is capable, in theory, of forming four isomeric [4 + 4] assemblies when combined with ditopic acceptor **1**. In the case of monochloro donor **3**, however, an even more complex set of isomeric metallacycles is possible depending upon the relative orientations of the α -Cl atoms within each square isomer (**A–D**). For example, isomer **A** of metallacycle **6** may have all α -Cl atoms aligned on the same face of the metallacycle, two on each side, or three on one side and one on the other (see Supporting Information for further details). Once assembled, the restricted rotation around the Pt–N bond¹² does not allow for α -Cl pyridyl moieties to rotate from one face of the square to the other. The varying size and location of substituents of **2–4** should play a key role in affecting product formation and, potentially, self-selection during self-assembly.¹³ It is important to note that the self-selectivity study described herein is different from previous reports that relied primarily upon geometric and electronic effects and utilized nonlinear ambidentate donor ligands. In the present study, all donors are linear and are the same length, precluding any geometric bias, and both coordination sites of each ligand are pyridyl nitrogen atoms, precluding a charge bias that arises when ambidentate ligands are used. In this Article we show that the series of unsymmetrical donors undergo various degrees of self-sorting due to the influence of steric and electronic effects during the self-assembly of [4 + 4] metallacyclic squares.

Results and Discussion

Supramolecular squares **5–7** were prepared by mixing 90° Pt(II) acceptor **1** with unsymmetrical donors **2–4**, respectively, in a 1:1 molar ratio in CD₃NO₂ at 298 K for 24 h. As previously discussed and shown in Scheme 1, four isomeric supramolecular squares of different symmetry may result from each self-assembly. The symmetry of each isomer must be carefully considered and correlated with NMR spectra in order to acquire structural details from spectroscopic studies. For each metal center coordinated by two different pyridyl moieties, the ³¹P{¹H} NMR of the PMe₃ ligands will appear as two coupled doublets given that the trans effect results in two inequivalent, and consequently coupled, phosphorus nuclei. Therefore, two doublets for the **A** isomer and two singlets for the **D** isomer will be observed in their corresponding ³¹P{¹H} NMR spectra because of the higher C₄ and D₂ symmetry of **A** and **D**, respectively. The ³¹P{¹H} NMR spectra of isomer **C** can be discerned, on the basis of its C₂ symmetry, as two coupled doublets along with two singlets. The low C_s symmetry of isomer **B** causes every phosphorus nucleus to be in a dissimilar chemical environment and can be identified as such. Accordingly, whether each self-assembly results in a single supramolecular square isomer or a randomly distributed mixture of possible isomers, NMR spectroscopic data can provide sufficient evidence for affirming the occurrence and efficiency of self-selection.

The reaction of **1** and **2** in CD₃NO₂ yields a homogeneous pale yellow solution of **5**. The ³¹P{¹H} NMR spectrum displays a pair of coupled doublets (CD₃NO₂, $\delta = -18.79$ ppm, ¹J_{Pt–P} = 3266.6 Hz, ²J_{P–P} = 23.8 Hz; $\delta = -25.94$ ppm, ¹J_{Pt–P} = 3578.4 Hz, ²J_{P–P} = 23.8 Hz) of approximately equal intensity with concomitant ¹⁹⁵Pt satellites (Figure 1a). Compared with the phosphorus NMR of the starting material **1** ($\delta = -20.09$ ppm, ¹J_{Pt–P} = 3915 Hz), the doublet of **5** at -18.79 ppm is shifted downfield by roughly 1.3 ppm, which can be assigned to the phosphorus nuclei trans to the dimethylpyridyl moiety, and forms a sharp contrast with the other doublet at $\delta = -25.94$ ppm, which is up-shifted about 5.8 ppm. This can be rationalized by the fact that the stronger electron-donating dimethylpyridyl moiety will weaken back-donation from the Pt(II) center to the opposite PMe₃ due to the trans effect. This deduction is further substantiated by the ¹H NMR spectra, in which the NMR signals

(12) (a) Fuss, M.; Siehl, H.-U.; Olenyuk, B.; Stang, P. J. *Organometallics* **1999**, *18*, 758–769. (b) Fan, J.; Whiteford, J. A.; Olenyuk, B.; Levin, M. D.; Stang, P. J.; Fleischer, E. B. *J. Am. Chem. Soc.* **1999**, *121*, 2741–2752. (c) Yamamoto, T.; Arif, A. M.; Stang, P. J. *J. Am. Chem. Soc.* **2003**, *125*, 12309–12317. (d) Chi, K.-W.; Addicott, C.; Arif, A. M.; Das, N.; Stang, P. J. *J. Org. Chem.* **2003**, *68*, 9798–9801. (e) Megyer, T.; Jude, H.; Grósz, T.; Bakó, I.; Radnai, T.; Tárkányi, G.; Pálinkás, G.; Stang, P. J. *J. Am. Chem. Soc.* **2005**, *127*, 10731–10738. (f) Tárkányi, G.; Jude, H.; Pálinkás, G.; Stang, P. J. *Org. Lett.* **2005**, *7*, 4971–4973. (g) Vacek, J.; Caskey, D. C.; Horinek, D.; Shoemaker, R. K.; Stang, P. J.; Michl, J. *J. Am. Chem. Soc.* **2008**, *130*, 7629–7638.

(13) (a) Yoshizawa, M.; Nagao, M.; Kumazawa, K.; Fujita, M. *J. Organomet. Chem.* **2005**, *690*, 5383–5388. (b) Rang, A.; Engeser, M.; Maier, N. M.; Nieger, M.; Lindner, W.; Schalley, C. A. *Chem. Eur. J.* **2008**, *14*, 3855–3859.

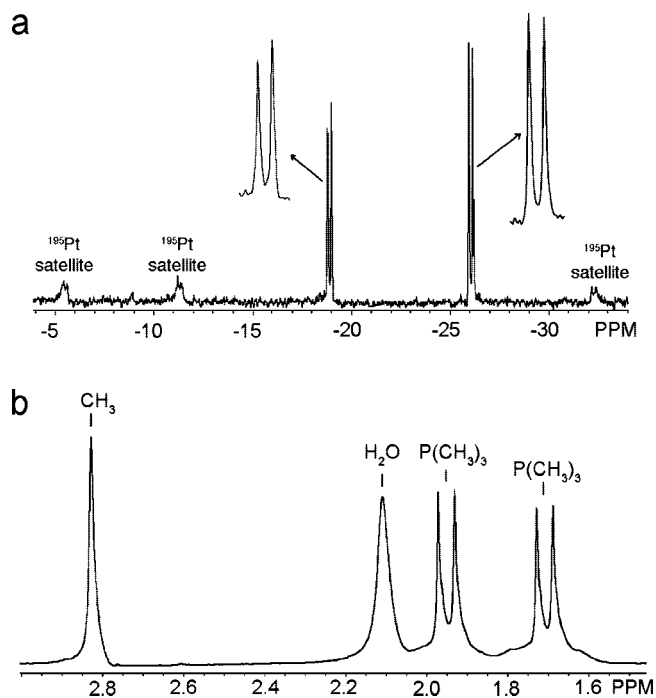


FIGURE 1. (a) Partial $^{31}\text{P}\{^1\text{H}\}$ NMR spectrum of **5** showing only two sets of doublets. (b) Partial ^1H NMR spectrum of **5** showing a set of coupled doublets arising from the two inequivalent PMe_3 substituents. The splitting pattern and high symmetry of both spectra strongly support the formation of only one isomer, isomer **A**, in the self-assembly of supramolecular square **5**.

attributed to the pyridyl α -Me groups of the PyMe_2 moiety, the β -H of PyMe_2 , and the β -H of the unsubstituted pyridine ring experienced downfield shifts of 0.32 ppm, 0.25 ppm and 0.32 ppm, respectively, much larger than the upfield shift of the α -H signals of the unsubstituted pyridine ring ($\Delta\delta = 0.02$ ppm), indicating the loss of electron density upon coordination of the unsubstituted pyridyl moiety to the Pt(II) center. Furthermore, two characteristic coupled doublets corresponding to different PMe_3 groups are also observed in the ^1H NMR spectrum at $\delta = 1.97$ and 1.73 ppm (Figure 1b), which exhibit a downshift of 0.11 ppm and an upshift by 0.13 ppm, respectively, relative to the PMe_3 proton signal of **1**. Consequently, the relative simplicity and symmetry of the coupled doublets in the $^{31}\text{P}\{^1\text{H}\}$ NMR spectrum of **5** are consistent with the formation of isomer **A**, showing that self-selection of one single isomer occurs in the self-assembly of **1** and unsymmetrical ligand **2**. Self-selection in the self-assembly of **5** is likely the result of interligand α -Me- α -Me steric interactions that prohibit the coordination of two of the dimethyl pyridyl moieties to the same Pt(II) center as well as electronic effects resulting from the difference in electron-donating abilities, as evidenced by NMR chemical shift changes, between the dimethyl pyridyl and pyridyl moieties of ligand **2**.

Mixing monochloro-substituted ligand **3** in a 1:1 stoichiometric ratio with acceptor **1** generates [4 + 4] self-assembly **6**. Sharp $^{31}\text{P}\{^1\text{H}\}$ and ^1H NMR spectroscopic peaks indicate that only discrete structures are obtained, however, the complicated splitting of $^{31}\text{P}\{^1\text{H}\}$ NMR spectrum suggest that multiple supramolecular isomers are formed. As shown in Figure 2, three pairs of doublets (blue: -26.59 ppm, -26.79 ppm, $^2J_{\text{P-P}} = 24.4$ Hz; red: -26.67 ppm, -26.87 ppm, $^2J_{\text{P-P}} = 24.4$ Hz; green: -26.92 ppm, -27.13 ppm, $^2J_{\text{P-P}} = 25.2$ Hz) are observed in the downfield region of the $^{31}\text{P}\{^1\text{H}\}$ NMR spectrum of **6**,

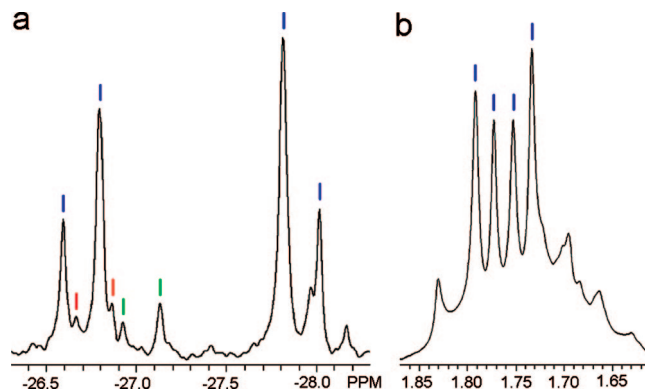


FIGURE 2. Partial $^{31}\text{P}\{^1\text{H}\}$ NMR (a) and ^1H NMR (b) spectra of the self-assembly of **6**. In both spectra, pairs of coupled doublets are indicated by blue, red, and green lines. On the basis of the splitting patterns, symmetry, and the intensities of spectral signals, it can be concluded that one predominant species (isomer **A**) is formed during self-assembly, though small amounts of other isomers are present as well.

indicating the existence of inequivalent coordination modes for the Pt(II) centers. The small difference of approximately 1.0 ppm between the downfield and upfield shifts of signals in the $^{31}\text{P}\{^1\text{H}\}$ NMR of **6** denotes similar electron density between the two pyridyl moieties, in contrast to the shifts observed for **5** (~ 7.0 ppm) where the difference in electron density is greater. A statistical analysis involving random variations of the orientation of donor ligands **3** within the supramolecular square **6** would suggest that the four possible isomers **A**:**B**:**C**:**D** would be formed in a 1:4:2:1 ratio in the absence of any interligand effects. However, the $^{31}\text{P}\{^1\text{H}\}$ NMR spectrum demonstrates that the single isomer corresponding to the doublet highlighted in blue is the dominant species in the mixture and the other two doublets (red and green) are of lower but roughly equal intensity. The PMe_3 signals in the ^1H NMR spectrum lend further support to the formation of one predominant isomer, one in which the two coupled doublets highlighted in blue at $\delta = 1.79$ ppm ($^2J_{\text{P-H}} = 5.7$ Hz) and 1.75 ppm ($^2J_{\text{P-H}} = 5.7$ Hz) have the same shape as those of assembly **5** and their symmetry implies that the resulting dominant species is also highly symmetric. The main species formed in the self-assembly of **6** can therefore be identified as isomer **A**. However, the monosubstitution of the less sterically bulky Cl atom and more similar electron-donating character of the monochloro and unsubstituted pyridyl moieties of **3** result in a decrease in the efficiency of self-selection in **6**

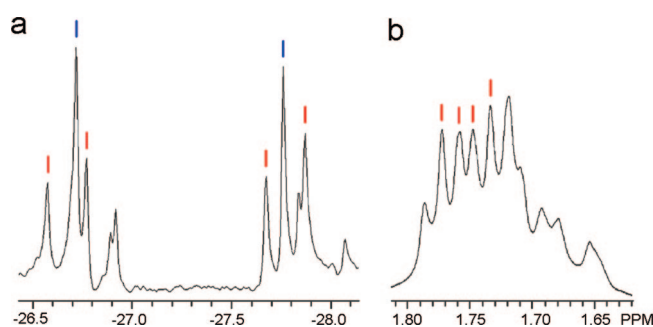


FIGURE 3. (a) Partial $^{31}\text{P}\{^1\text{H}\}$ NMR spectrum of self-assembly **7**. Pairs of coupled doublets are indicated by red and blue lines. (b) Partial ^1H NMR spectrum of self-assembly **7**. The set of two coupled doublets highlighted by red lines corresponds to the same species that gives rise to the coupled doublets (red) in the $^{31}\text{P}\{^1\text{H}\}$ NMR spectrum and can be ascribed to isomer **A**.

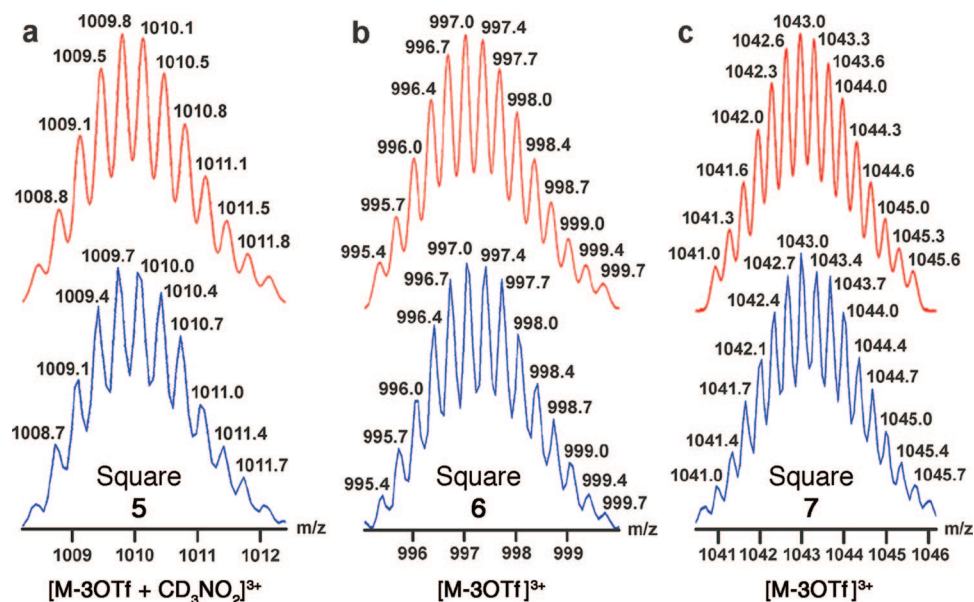


FIGURE 4. Theoretical (top, red) and experimental (bottom, blue) ESI-MS of self-assembled squares (a) **5** $[M - 3OTf + CD_3NO_2]^{3+}$, (b) **6** $[M - 3OTf]^{3+}$, (c) **7** $[M - 3OTf]^{3+}$.

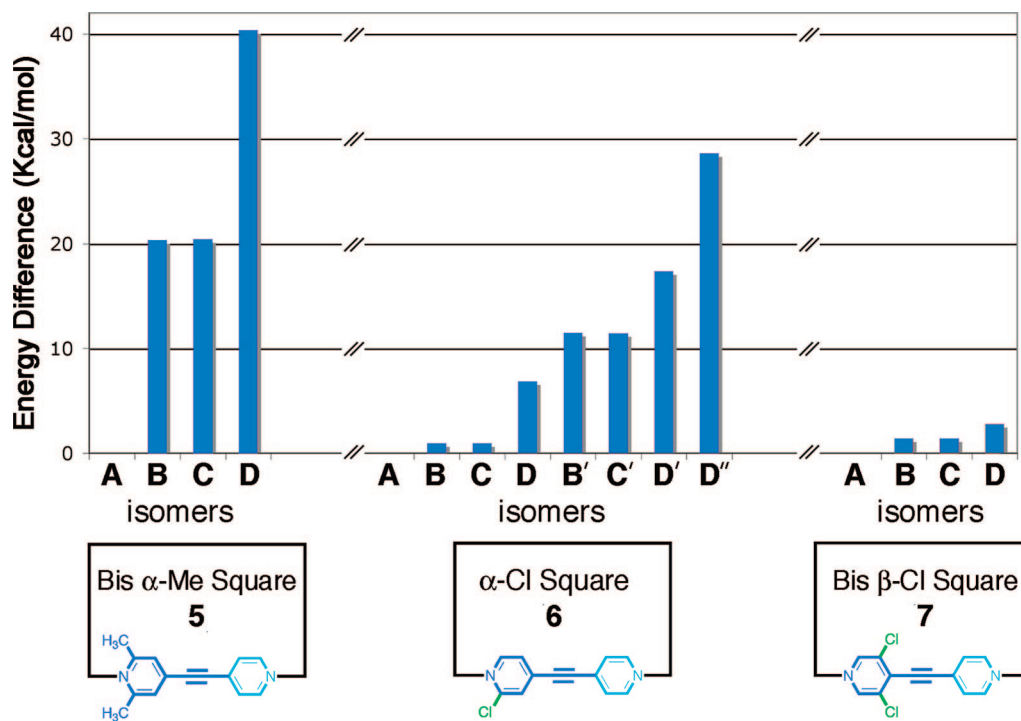


FIGURE 5. Graph of the energy differences between isomers A–D of supramolecular squares **5**–**7** obtained from molecular modeling. Energies are expressed in Kcal/mol. For all squares (**5**, **6**, and **7**), isomer A was found to be the most stable and is therefore listed as 0.0 Kcal/mol. The energies of isomers B–D of square **5** are given relative to isomer A of square **5** and so on for each supramolecular square. For the α -Cl square **6**, isomers indicated with a prime (') are secondary structural isomers with α -Cl atoms on the same face of **6**, as discussed in the text.

relative to the high degree of self-selection observed in the self-assembly of **5**.

To investigate the steric interactions between substituents at the β position of the pyridyl moieties and their effect on self-selection, we mixed dichloro donor ligand **4** with acceptor **1** in a 1:1 stoichiometric ratio, thus yielding a colorless solution of **7**. The resulting ^{31}P NMR spectrum is significantly more complex than those of **5** and **6**, with most peaks having near equal intensity. One pair of singlets (blue) and one pair of coupled doublets (red) can be distinguished as shown in Figure 3. The coupled doublets (red) are located at $\delta = -26.58$ ppm

($^2J_{P-P} = 23.8$ Hz) and -27.67 ($^2J_{P-P} = 23.8$ Hz). These $^{31}P\{^1H\}$ NMR signals relate to the pair of coupled signals highlighted in red that are observed in the 1H NMR spectrum at $\delta = 1.77$ ppm ($^2J_{P-H} = 4.2$ Hz) and 1.75 ($^2J_{P-P} = 4.5$ Hz). By analogy to the NMR spectrum and analysis of **6**, it is clear that such coupled doublets (red) in the $^{31}P\{^1H\}$ and 1H NMR spectra of **7** can be attributed to isomer A. Unlike self-assemblies **5** and **6**, however, the intensities of peaks associated with the A isomer of **7** are almost equivalent to adjacent peaks. Due to significant overlapping of signals in both the ^{31}P and 1H NMR spectra, it is difficult to determine which other isomers (B–D) are present

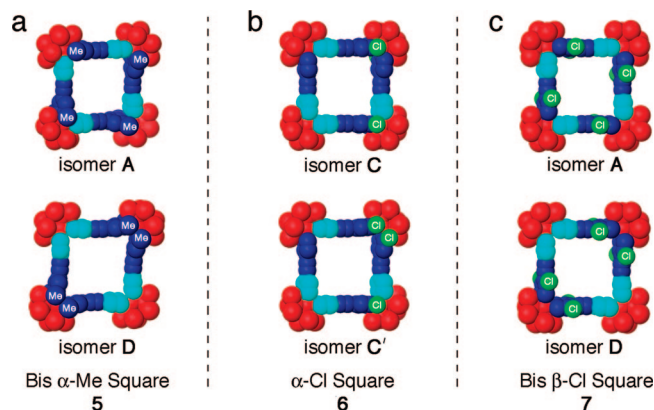


FIGURE 6. Representative examples of isomers of supramolecular squares **5** (a), **6** (b), and **7** (c) obtained from molecular force field modeling. Methyl and chloro substituents on the “front” face of each square are labeled as “Me” or “Cl.” The difference in steric interactions between isomers **A** and **D** of bis α -Me square **5** can be seen in (a). In (b) is an example of secondary isomers that are possible in α -Cl square **6**: isomer **C** (top) has all four Cl atoms on alternating faces of the square, whereas isomer **C'** (bottom) has two Cl atoms coordinated to the same Pt(II) center on the same face of the square, inducing steric and electrostatic repulsion. The structural differences between isomers **A** and **D** of bis β -Cl square **7** in (c) are very minor, giving rise to a difference of only 2.7 Kcal/mol between the two isomers.

in the mixture and in what relative amounts. These observations indicate that the β -dichloro substituted ligand (**4**) has considerably less influence on the self-selection of a single isomer because the two chlorine atoms are too far removed from the Pt–N coordination site to have significant steric or electronic influence.

The formation of discrete supramolecular squares during the self-assembly of **5–7** is further confirmed by electrospray ionization mass spectrometry (ESI-MS). As shown in Figure 4, the peaks resulting from each self-assembly after the loss of three triflate anions are found at [**5** – 3CF₃SO₃[–] + CD₃NO₂]³⁺ (*m/z* 1009.7), [**6** – 3CF₃SO₃[–]]³⁺ (*m/z* 997.0) and [**7** – 3CF₃SO₃[–]]³⁺ (*m/z* 1043.0). It is noteworthy that one nitromethane molecule is consistently found in the ionization species of self-assembly **5** though not in the other two **6** and **7**. This is likely the result of the high boiling point of CD₃NO₂ and from C–H···O hydrogen-bonding interactions between the pyridyl methyl moieties and CD₃NO₂, an interaction not present in assemblies **6** and **7**. All observed peaks are isotopically resolved and in good agreement with their corresponding theoretical distributions (red). ESI-MS results unambiguously identify **5–7** as [4 + 4] supramolecular squares; however, they cannot distinguish the relative abundances of different isomers of each square.

Molecular force field modeling was used to investigate the differences between the **A–D** isomers of supramolecular squares **5–7** and to gain insight into the preference, if any, for forming one isomer at the expense of others. Each individual isomer of squares **5–7** was built within the input mode of the program Maestro v9.51.09 and subjected to a 1 ns molecular dynamics simulation (MMFF force field, gas phase, 300 K) in order to equilibrate the structures. The output of each simulation was then minimized to full convergence. In every case it was found that isomer **A** of supramolecular squares **5–7** was the lowest energy and therefore the most favored isomer. A comparison of the energy differences between isomers **B–D** relative to isomer **A** (taken as the zero point of relative energy for each

assembly) is shown in Figure 5 for each respective supramolecular square **5–7**. These energy differences of isomers **A–D** provide strong support for the experimental NMR spectroscopic results. In the case of self-assembly **5**, for example, only one isomer is observed spectroscopically. Molecular modeling suggests a large difference in energy between isomer **A** of self-assembly **5** and the other isomers (**B**, **C**: 20.3 kcal/mol; **D**: 40.3 kcal/mol) on account of unfavorable interligand Me–Me steric interactions between ligands oriented such that their pyridyl α -methyl groups are coordinated to the same Pt(II) center. These steric effects occur at one Pt(II) center in isomers **B** and **C** and at two Pt(II) centers for isomer **D**, which accounts for the trend in the energy differences. As a result of interligand Me–Me interactions, isomer **D** must distort to adopt a more rhomboidal shape as shown in Figure 6a.

As mentioned previously, a number of secondary structural isomers are possible for self-assembled supramolecular square **6** due to the reduced symmetry of linear donor **3** compared to donors **2** and **4**. The four pyridyl α -Cl atoms may align all on one side of square **6**, two on each side, or three on one side and one on the other. Those isomers having α -Cl atoms coordinated to the same Pt(II) center and on the same face of **6** experience repulsive interligand (α -Cl)–(α -Cl) steric and electronic interactions and have higher relative energies than those having the α -Cl atoms on opposite faces of the supramolecular square. An example comparing the **C** and **C'** isomers of **6** is shown in Figure 6b. Molecular modeling indicates that the **B** and **C** isomers having α -Cl atoms of pyridyl moieties attached to the same Pt(II) center but oriented on opposite faces of the square have mean relative energies of about 0.9 Kcal/mol compared to isomer **A**. In the case of isomer **D**, the lowest energy conformation (that with α -Cl atoms on alternating faces of square **6**) is 6.8 Kcal/mol above isomer **A**. This decrease in relative energy differences between isomers **A**, **B**, **C**, and **D** is in contrast to those observed for supramolecular square **5** and is in agreement with the observation that a limited self-selection process occurs in the self-assembly of **6**. Isomers with adjacent α -Cl atoms on the same face of square **6** (i.e., **B'**, **C'**, **D'**, and **D''**; see Supporting Information) have higher relative energies ranging from 11.4 to 28.5 Kcal/mol above the lowest energy isomer **A**. Lastly, when the substituents are moved far away from the Pt–N bonding center as they are in square **7** (Figure 6c), the relative energy gaps between **A** and **B–D** are all within 2.7 Kcal/mol, too small to efficiently control the self-selection process, thus generating a mixture of many isomers.

In summary, we have utilized steric effects between substituents of unsymmetrical bis(4-pyridyl)acetylene ligands (**2–4**) to control the degree of self-selection in the self-assembly of [4 + 4] supramolecular squares. The collective ³¹P and ¹H NMR spectra indicate that the efficiency of self-selection of isomers is greater when substituents of greater steric bulk are located at positions proximal to the Pt–N bonding motif and efficiency decreases as the size of substituents is decreased or the substituents are moved further from the Pt–N coordination site. Molecular modeling using the MMFF force field allows for the relative energy of each isomer of the supramolecular squares to be compared, and the results support the experimental trend in self-selectivity from complete self-selectivity, as in supramolecular square **5**, to the absence of self-selectivity, as in supramolecular square **7**.

Experimental Section

Methods and Materials. The organoplatinum acceptor ligand *cis*-(PMe₃)₂Pt(OTf)₂ (**1**) was synthesized according to literature methods.¹⁴ 2-Chloro-4-iodopyridine and 3,5-dichloro-4-iodopyridine were purchased from Aldrich and used without further purification. 4-Bromo-2,6-lutidine was prepared according to published procedure.¹⁵ 4-Ethynylpyridine was freshly prepared prior to a reaction by neutralization of commercially available its HCl salt.

General Method for Synthesis of Unsymmetrical Bipyridyl Ligands 2–4. A 10-mL Schlenk flask was charged with 4-ethynylpyridine (0.20 mmol), aryl halide (0.20 mmol), bis(triphenylphosphine) palladium(II) dichloride (0.005 mmol) and copper(I) bromide (0.009 mmol) under a stream of nitrogen. Freshly distilled triethylamine (3 mL) was added to the flask via syringe, and the reaction mixture was stirred for 24 h at 80–90 °C. The solvent was then evaporated in vacuo, and the resulting residue was dissolved in CH₂Cl₂ (50 mL). The organic phase was washed with saturated aqueous NaHCO₃ (15 mL) and dried over anhydrous Na₂SO₄. Purification by column chromatography with silica gel yields the corresponding unsymmetrical bipyridyl ligands.

2,6-Dimethyl-4-(pyridin-4-ylethynyl)pyridine (2). Dark brown solid, 32% yield, mp 157–160 °C; ¹H NMR (300 MHz, CDCl₃) δ 2.51 (s, 6H), 7.29 (s, 2H), 7.34 (dd, *J* = 4.5, 1.5 Hz, 2H), 8.61 (dd, *J* = 4.5, 1.5 Hz, 2H); ¹³C NMR (75 MHz, CDCl₃) δ 18.4, 90.7, 91.0, 118.0, 125.7, 126.6, 130.8, 149.3, 149.9; MS(EI) 208(M+, 100), 192(15), 180(10), 166(7), 77(10), 51(8). Anal. Calcd for C₁₄H₁₂N₂: C, 80.74; H, 5.81; N, 13.45. Found: C, 80.31; H, 5.50; N, 13.22.

2-Chloro-4-(pyridin-4-ylethynyl)pyridine (3). Pale yellow solid, 69% yield, mp 110–112 °C; ¹H NMR (300 MHz, CDCl₃) δ 7.31 (dd, *J* = 5.1, 1.2 Hz, 1H), 7.38 (dd, *J* = 4.5, 1.5 Hz, 2H), 7.45 (s, 1H), 8.40 (d, *J* = 5.1 Hz, 1H), 8.64 (dd, *J* = 4.5, 1.5 Hz, 2H); ¹³C NMR (75 MHz, CDCl₃) δ 89.4, 92.1, 124.5, 125.8, 126.4, 129.9, 133.2, 150.0, 150.2, 152.1; MS(EI) 216(41), 214(M+, 100), 179(65), 152(16), 126(10), 99(11), 74(11), 51(5). Anal. Calcd for C₁₂H₇ClN₂: C, 67.15; H, 3.29; N, 13.05. Found: C, 67.05; H, 3.23; N, 12.71.

3,5-Dichloro-4-(pyridin-4-ylethynyl)pyridine (4). White solid, 31% yield, mp 169–171 °C; ¹H NMR (300 MHz, CDCl₃) δ 7.47 (dd, *J* = 4.5, 1.5 Hz, 2H), 8.55 (s, 2H), 8.68 (dd, *J* = 4.5, 1.5 Hz, 2H); ¹³C NMR (75 MHz, CDCl₃) δ 85.0, 100.9, 125.9, 129.7, 129.8, 133.7, 147.3, 150.3; MS(EI) 252(12), 250(64), 248(M+, 100), 213(20), 186(12), 151(14), 124(12), 98(15), 74(7). Anal. Calcd for C₁₂H₆Cl₂N₂: C, 57.86; H, 2.43; N, 11.25. Found: C, 57.60; H, 2.38; N, 10.87.

Self-Assembly of Square 5. A CD₃NO₂ solution of 2,6-dimethyl-4-(pyridin-4-ylethynyl)pyridine **2** (1.85 mg, 8.88 μmmol) was transferred into a vial charged with a 0.2 mL CD₃NO₂ solution of *cis*-(Me₃P)₂Pt(OTf)₂ **1** (5.73 mg, 8.88 μmmol) and washed with excess CD₃NO₂ (3 × 0.15 mL) to ensure quantitative transfer. The mixture was stirred for 24 h to generate a clear pale yellow solution, which was then placed into a NMR tube for analysis. Evaporating

the solvent under a vacuum pump resulted in the solid product. Yield: 95%. ¹H NMR (CD₃NO₂, 300 MHz): δ 8.65 (m, 8H, H_α-Py), 7.68 (d, *J* = 5.7 Hz, 8H, H_β-Py), 7.54 (s, 8H, H_β-Py), 2.83 (s, 24H, CH₃-Py), 1.97 (d, ²J_{P-H} = 12 Hz, 36H, PCH₃), 1.73 (d, ²J_{P-H} = 12 Hz, 36H, PCH₃). ³¹P {¹H} NMR (CD₃NO₂, 121.4 MHz): δ -18.79 (d, ¹J_{Pt-P} = 3266.6 Hz, ²J_{P-P'} = 23.8 Hz), -25.94 (d, ¹J_{Pt-P} = 3578.4 Hz, ²J_{P-P'} = 23.8 Hz).

Self-Assembly of Square 6. The dipyrindyl donor ligand 2-chloro-4-(pyridin-4-ylethynyl)pyridine **3** (2.17 mg, 10.10 μmmol) and the organoplatinum 90° acceptor *cis*-(Me₃P)₂Pt(OTf)₂ **1** (6.52 mg, 10.10 μmmol) were weighed and added to respective glass vials. The vial containing donor ligand **3** was charged with 0.2 mL of CD₃NO₂ solvent, which was subsequently transferred to the vial filled with a 0.2 mL CD₃NO₂ solution of **1**. This process was repeated three times (3 × 0.15 mL) to ensure quantitative transfer of the donor to the acceptor. The reaction solution was then stirred at room temperature for 24 h to yield a homogeneous colorless solution. The solution was transferred into the NMR tube to collect ¹H and ³¹P NMR spectra. Solid product was obtained by removing the solvent under vacuum pump. Yield: 96%. ¹H NMR (CD₃NO₂, 300 MHz): δ 8.96–9.02 (m, 12H, H_α- and H_α-Py), 7.76–7.98 (m, 16H, H_β- and H_β-Py), 1.66–1.83 (m, 72H, PCH₃). ³¹P {¹H} NMR (CD₃NO₂, 121.4 MHz): δ -26.59 - -27.13 (three doublets, ¹J_{Pt-P} = 3302.8 Hz; -26.59, -26.79, ²J_{P-P'} = 24.4 Hz; -26.67, -26.87, ²J_{P-P'} = 24.4 Hz; -26.92, -27.13, ²J_{P-P'} = 25.2 Hz), -27.82 - -28.17 (two doublets, ¹J_{Pt-P} = 3142.8 Hz; -27.82, -28.02, ²J_{P-P'} = 24.4 Hz; -27.97, -28.17, ²J_{P-P'} = 24.4 Hz).

Self-Assembly of Square 7. To a 0.2 mL CD₃NO₂ solution of *cis*-(Me₃P)₂Pt(OTf)₂ **1** (6.01 mg, 9.31 μmmol) in a vial was added a 0.2 mL CD₃NO₂ solution of 3,5-dichloro-4-(pyridin-4-ylethynyl)pyridine **4** (2.32 mg, 9.31 μmmol). This process was repeated three times (3 × 0.15 mL) to complete transfer of the donor to the acceptor. The reaction mixture was stirred at ambient temperature for 24 h to produce a clear colorless solution. The solution was transferred into the NMR tube for ¹H and ³¹P NMR spectra collection. The solid product was obtained by removing CD₃NO₂ under vacuum. Yield: 93%. ¹H NMR (CD₃NO₂, 300 MHz): δ 8.98–9.28 (m, 16H, H_α- and H_α-Py), 7.82–7.89 (m, 8H, H_β-Py), 1.65–1.79 (m, 72H, PCH₃). ³¹P {¹H} NMR (CD₃NO₂, 121.4 MHz): δ -26.58 - -26.92 (m, ¹J_{Pt-P} = 3284.1 Hz), -27.67 - -28.07 (m, ¹J_{Pt-P} = 3156.1 Hz).

Acknowledgment. P.J.S. thanks the NIH (Grant GM-057052) and the NSF (Grant CHE-0306720) for financial support. B.H.N. thanks the NIH (Grant GM-080820) for financial support. This work was also supported by the 2008 Research Fund of the University of Ulsan.

Supporting Information Available: ¹H and ¹³C NMR spectroscopic characterization of unsymmetrical ligands (**2–4**), ³¹P and ¹H NMR spectra of assemblies **5–7**, and description of secondary isomers of assembly **6**. This material is available free of charge via the Internet at <http://pubs.acs.org>.

JO800957R

(14) Stang, P. J.; Cao, D. H.; Saito, S.; Arif, A. M. *J. Am. Chem. Soc.* **1995**, *117*, 6273–6283.

(15) Evans, R. F.; Brown, H. C. *J. Org. Chem.* **1962**, *27*, 1665–1667.